Stress distribution in a plate subject to uniaxial loading
Beale, S.B.; Elias, S.R.

Publisher's version / Version de l'éditeur:

The PHOENICS journal of computational fluid dynamics and its applications, 3, 3, pp. 255-287, 1990

MARIA CLANCY
DGO
INST FOR CHEM PROCESS & ENVIR TECH
NATIONAL RESEARCH COUNCIL CANADA
M-12, ROOM 141, 1200 MONTREAL RD.
OTTAWA, ON K1A 0R6
CANADA

ORDER NUMBER:	**CI-07531487-3**
Account Number:	WR001844
Delivery Mode:	XLB
Delivery Address:	
Submitted:	2008/08/01 14:24:22
Received:	2008/08/01 14:24:22
Printed:	2008/08/01 22:43:00

Extended **Periodical** **WWW Blank** **CANADA**

Title:	**PHOENICS JOURNAL OF COMPUTATIONAL FLUID DYNAMICS**
Vol./Issue:	3/3/OCTOBER
Date:	1990
Pages:	255-287
Article Title:	STRESS DISTRIBUTION IN A PLATE SUBJECT TO UNIAXIAL LOADING
Article Author:	S.B. BEALE AND S.R. ELIAS

Estimated cost for this 33 page document: $0 document supply fee + $0 copyright = $0

ɔfessor D Brian Spalding FRS
Norberto Fueyo
s Sylvie Stevens

ɫAM Limited
kery House
High Street
mbledon SW19 5AU
gland

1 947 7651
1 879 3497
8517

ıarterly

5.00 per annum, including surface mail
stage (overseas £55).

7.50 per copy (£20 for airmail).

STRESS DISTRIBUTION IN A PLATE SUBJECT TO UNIAXIAL LOADING

by

S.B. Beale
Institute for Mechanical Engineering,
National Research Council,
Ottawa, Ontario, Canada K1A 0R6

and

S. R Elias
Department of Mechanical Engineering
University of Waterloo,
Waterloo, Ontario, Canada N2L 3G1

This contribution was submitted to the PHOENICS journal in October 1990. The work was conducted using PHOENICS Version 1.4 on a DEC Local Area VAX-cluster, and also using NISA2 on an IBM 3090.

ABSTRACT

This paper shows how the methods of computational fluid dynamics may be used to solve two-dimensional solid mechanics problems, using an analogy which exists between plane elasticity and creeping flow. A problem involving a rectangular plate subject to uniaxial loading is considered in detail. The stress distribution obtained using PHOENICS is compared with that obtained using the finite-element analysis package NISA2. The results and potential for application are discussed in detail.

1. 0 OBJECTIVE OF THE WORK

Computational fluid dynamics (CFD) has made rapid progress in the last two decades. It is now possible to generate precise solutions to complex problems involving fluid flow, heat and mass transfer. The development of finite element analysis (FEA) has also resulted in the solution of numerous problems in structural analysis. FEA codes have been applied to a number of other phenomena, including fluid flow and heat transfer. At the present time, however, most general-purpose CFD codes, such as PHOENICS, are based on the finite-domain formulation, using algorithms derived from SIMPLE (Patankar and Spalding, 1972).

The purpose of this project was to demonstrate that a conventional finite-domain based CFD code may be successfully used to solve elasticity problems. The scope of the work is confined to two-dimensional problems with constant properties and no body forces. Use is made of a well known analogy between the state of stress of an elastic solid, and the behaviour of a fluid flowing at negligible Reynolds' numbers.

The solid-fluid analogy was discussed in detail by Goodier (1934). Since then, complex function theory has been used to solve a number of problems of academic interest (e.g. Dean, 1958) in both creeping flow, and plane elasticity. More recently, Johnston and Tabarrok (1978) exploited the fluid-solid analogy in order to solve 2-D fluid flow problems by finite-element methods.

The immediate goal of this project was the converse; namely the solution of plane elastic problems using conventional methods of CFD, ie., by solving the pressure-linked hydrodynamic equations. It is hoped that the methodology may be subsequently extended to develop a rationale for the simultaneous solution of fluid mechanics and structural engineering problems, using a single computer code. This paper is specifically directed toward the PHOENICS user, and is an abridged version of a report by Beale and Elias (1990), which contains additional details.

ıas made rapid progress in the last two decades. It
utions to complex problems involving fluid flow,
ıent of finite element analysis (FEA) has also re-
ɔlems in structural analysis. FEA codes have been
na, including fluid flow and heat transfer. At the
ırpose CFD codes, such as PHOENICS, are based
ʒ algorithms derived from SIMPLE (Patankar and

nonstrate that a conventional finite-domain based
ı solve elasticity problems. The scope of the work
ms with constant properties and no body forces.
between the state of stress of an elastic solid, and
ligible Reynolds' numbers.

in detail by Goodier (1934). Since then, complex
: a number of problems of academic interest (e.g.
nd plane elasticity. More recently, Johnston and
lid analogy in order to solve 2-D fluid flow prob-

s the converse; namely the solution of plane elas-
ds of CFD, ie., by solving the pressure-linked hy-
t the methodology may be subsequently extended
ous solution of fluid mechanics and structural en-
ıputer code. This paper is specifically directed to-
abridged version of a report by Beale and Elias
ls.

2. 0 DESCRIPTION OF THE PROBLEM

2.1 Sample problem

The problem considered was a thin rectangular plate (aspect ratio 2:1) subject to two point forces acting along the centreline [Fig. 1]. This example was analyzed using both the finite-domain code PHOENICS, and also the finite-element program NISA2 (Mathers, 1983).

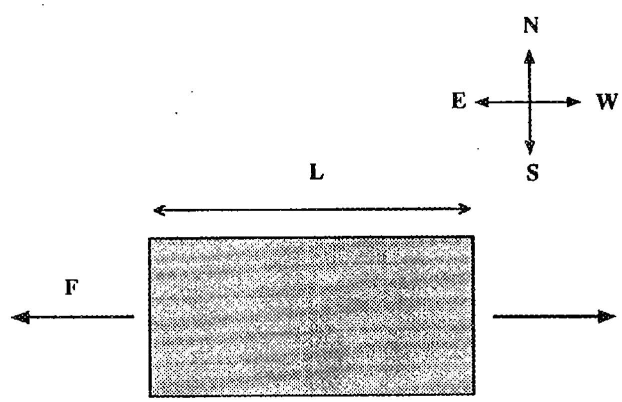

Figure 1. Sample problem

2.2 Mathematical details

2.2.1 Linear elastic solid

The equilibrium equations for a body in a state of plane stress or plane strain may be written as,

$$\frac{\partial \sigma_{xx}}{\partial x} + \frac{\partial \sigma_{xy}}{\partial y} + F_x = 0 \tag{1}$$

$$\frac{\partial \sigma_{xy}}{\partial x} + \frac{\partial \sigma_{yy}}{\partial y} + F_y = 0 \tag{2}$$

where σ_{xx}, σ_{yy} and σ_{xy} are the components of the stress tensor, and F_x and F_y are the body force components. Compatibility requires that,

$$\nabla^2 \zeta = 0 \tag{3}$$

where,

$$\zeta = \sigma_{xx} + \sigma_{yy} \tag{4}$$

so that ζ is harmonic, ie. satisfies Laplace's Equation. ζ ,may be considered to be the real part of a complex harmonic potential function, W, given by

$$W = \zeta + i\,\eta \tag{5}$$

The functions ζ and η are conjugate functions, so that they form families of mutually orthogonal curves

It can be shown that under these circumstances, all stress-related quantities may be derived from a single scalar function, ϕ. This function is named the Airy stress function, and has has been utilized extensively in two-dimensional stress analysis, the reader is referred to numerous texts (Chou and Pagano, 1967, Little, 1973, Muskhelishivili, 1953, Timoshenko, 1934). In the absence of body forces, it can be shown that the stress function is biharmonic,

$$\nabla^4 \phi = 0 \tag{6}$$

$$+\frac{\partial \sigma_{xy}}{\partial y} + F_x = 0 \qquad (1)$$

$$+\frac{\partial \sigma_{yy}}{\partial y} + F_y = 0 \qquad (2)$$

onents of the stress tensor, and F_x and F_y are the requires that,

$$\nabla^2 \zeta = 0 \qquad (3)$$

$$= \sigma_{xx} + \sigma_{yy} \qquad (4)$$

place's Equation. ζ ,may be considered to be the ial function, W, given by

$$W = \zeta + i\,\eta \qquad (5)$$

functions, so that they form families of mutually

ımstances, all stress-related quantities may be de- This function is named the Airy stress function, in two-dimensional stress analysis, the reader is Pagano, 1967, Little, 1973, Muskhelishivili, 1953, body forces, it can be shown that the stress func-

$$\nabla^4 \phi = 0 \qquad (6)$$

2.2.2 Creeping viscous flow

The scope of the analysis is restricted to the steady two-dimensional flow of an incompressible fluid with constant properties. The very slow flow of a linear viscous fluid is referred to as creeping flow (for an introduction to creeping flow, the reader is referred to Langlois, 1964) Under these conditions, the influence of inertia is negligible, so that the momentum equations are dominated by viscous and pressure gradient terms only;

$$\frac{\partial p}{\partial x} = \mu \nabla^2 u \qquad (7)$$

$$\frac{\partial p}{\partial y} = \mu \nabla^2 v \qquad (8)$$

Equations (7) and (8) are known as Stokes' equations.

Continuity requires that,

$$\frac{\partial u}{\partial x} + \frac{\partial v}{\partial y} = 0 \qquad (9)$$

In any two-dimensional flow problem, it is possible to show that the velocity components may be derived from a scalar stream function, ψ, and that, for creeping flow, the stream function is biharmonic. It can also be shown that both the vorticity, ξ , and the ratio of the pressure to viscosity, p/μ are harmonic, so that they may be considered to be the real and imaginary parts of a complex potential, given by;

$$W = -\xi - i\frac{p}{\mu} \qquad (10)$$

It is important to note that, since p/μ and ξ are conjugate, lines of constant pressure are lines of zero vorticity flux (gradient) and visa-versa.

2.2.3 The Solid-Fluid Analogy

Because the stress function and the stream function both satisfy the biharmonic equation, it is evident that an analogy exists between a linear elastic solid in a state of plane stress or plane strain, and the two-dimensional creeping flow of a linear viscous fluid.

From the point-of-view of this study, the independent elastic variables are considered to be the three stress components σ_{xx}, σ_{yy}, and σ_{xy} . (However, it is also possible to consider the strain components ε_{xx}, ε_{yy}, and ε_{xy}, or the displacements U_x, and U_y to be the fundamental variables). In fluid mechanics, it is the two velocity components, *u* and *v*, and the pressure, *p*, which are required. Since both the equilibrium and compatibility equations (1) - (3) and the momentum and continuity equations (7) - (9) are derivable from biharmonic equations, they may be considered functionally equivalent.

Table 1 is a summary of the correspondence of variables in the two cases. The reader will note that the correspondence is not dimensionally equivalent. The components of the elastic stress tensor[1] correspond to velocity gradients in the analogue, in such a fashion that the magnitude of the fluid vorticity is equal to (the negative of) the sum of the normal elastic stresses The interpretation of the elastic analogue to the pressure is indirect; isobars are families of curves perpendicular to the vorticity, ξ, the same is true for η with respect to the sum of the normal stresses

[1] Throughout this text, the term 'stress' is applied exclusively in the context of an elastic solid, while the term 'pressure' applied only to a viscous fluid. It is thus hoped to avoid any ambiguity which might otherwise arise.

stream function both satisfy the biharmonic equa-
ists between a linear elastic solid in a state of plane
nensional creeping flow of a linear viscous fluid.

, the independent elastic variables are considered to
σ_{yy}, and σ_{xy} . (However, it is also possible to con-
, and ε_{xy}, or the displacements U_x, and U_y to be the
chanics, it is the two velocity components, *u* and *v*,
ired. Since both the equilibrium and compatibility
ım and continuity equations (7) - (9) are derivable
y be considered functionally equivalent.

ondence of variables in the two cases. The reader
not dimensionally equivalent. The components of
o velocity gradients in the analogue, in such a fash-
orticity is equal to (the negative of) the sum of the
ation of the elastic analogue to the pressure is indi-
erpendicular to the vorticity, ξ, the same is true for
ıal stresses

plied exclusively in the context of an elastic solid, while the
uid. It is thus hoped to avoid any ambiguity which might oth-

Table 1 Elastic solid - viscous fluid analogy

ELASTIC SOLID		VISCOUS FLUID	
Quantity	**(Units)**	**Quantity**	**(Units)**
φ	(N.m)	ψ	(m^3/s)
$\partial\varphi/\partial y$	(N)	u	(m/s)
$-\partial\varphi/\partial x$	(N)	v	(m/s)
σ_{xx}	(N/m^2)	$\partial u/\partial y$	(s^{-1})
σ_{yy}	(N/m^2)	$-\partial v/\partial x$	(s^{-1})
σ_{xy}, σ_{yx}	(N/m^2)	$\partial v/\partial y, -\partial u/\partial x$	(s^{-1})
η	(N/m^2)	$-p/\mu$	(s^{-1})
ζ	(N/m^2)	$-\xi$	(s^{-1})

2.2.4 Boundary conditions

Although only force boundary conditions are considered in the example presented in this paper, some discussion of other boundary conditions is worthwhile. The types of boundary condition which may be readily converted to fluid-type boundary conditions are (a) Constant normal stress, (b) Constant shear stress, (c) Force, and (d) Bending moment. These are discussed below.

(a) Constant Normal Stress:

With reference to Figure 2 (a), it is observed that for constant normal stress, σ_n, acting on a flat surface perpendicular to the x axis, the corresponding flow is a shear distribution of the u velocity in the y direction, ie. the velocity boundary value is in the form of a ramp profile.

(b) Constant Shear Stress:

The velocity distribution resulting from a constant shear stress, σ_t, is shown in Figure 2 (b). In this case, there is a source of v-momentum in the x-direction. The source exhibits dilatation in the y-direction. Shear stresses always act on all four sides of an element, so that there is also a u-momentum distribution in the y-direction which exhibits compression in the x-direction.

(c) Force:

A normal force acting at a point may be regarded as the limiting case of a constant stress boundary condition. It is therefore evident that in this case, the associated velocity distribution is in the form of a step function [Fig. 2(c)]. The magnitude of the step is equal to that of the force. A shear force may be similarly considered as the limiting of case (b), above.

(d) Bending Moment:

Bending moments effect boundary conditions of a somewhat different nature: The bending stresses associated with moments are calculated using elementary Euler-Bernoulli beam theory. These are then equated with velocity gradients. It can be shown (eg. Little, 1973) that these equations also correspond to exact solutions under the assumptions of plane stress and plane strain. The bending stresses are,

$$\sigma^b_{xx} = -\frac{M_x y}{I_y} \tag{11}$$

$$\sigma^b_{yy} = -\frac{M_y x}{I_x} \tag{12}$$

where M_x, M_y = Moment about x or y axis

x, y = Distance from neutral axis

I_x, I_y = Moment of Inertia about x or y axis

Under the combined influence of surface traction and bending moments, the velocity gradients are obtained by superposition, s:

om a constant shear stress, σ_t, is shown in Figure 2 v-momentum in the x-direction. The source exhibits tresses always act on all four sides of an element, so tribution in the y-direction which exhibits compres-

be regarded as the limiting case of a constant stress vident that in this case, the associated velocity distri- on [Fig. 2(c)]. The magnitude of the step is equal to be similarly considered as the limiting of case (b),

onditions of a somewhat different nature: The bend- its are calculated using elementary Euler-Bernoulli l with velocity gradients. It can be shown (eg. Little, espond to exact solutions under the assumptions of ending stresses are,

$$\sigma^b_{xx} = -\frac{M_x y}{I_y} \quad (11)$$

$$\sigma^b_{yy} = -\frac{M_y x}{I_x} \quad (12)$$

= Moment about x or y axis

= Distance from neutral axis

= Moment of Inertia about x or y axis

urface traction and bending moments, the velocity ion,

$$\frac{\partial u}{\partial y} = \sigma_{xx} - \frac{M_x y}{I_y} \quad (13)$$

$$\frac{\partial v}{\partial x} = -\sigma_{yy} + \frac{M_y x}{I_x} \quad (14)$$

The velocity boundary condition resulting from a bending moment is therefore in the form of a parabolic distribution [Figure 2 (d)].

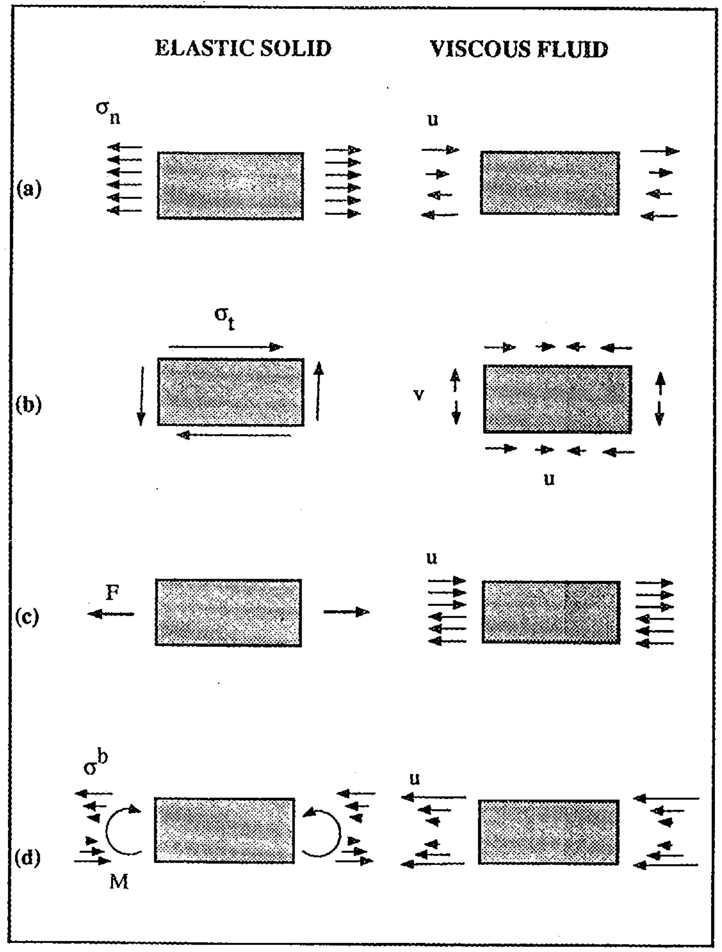

Figure 2. **Solid/fluid boundary conditions.**

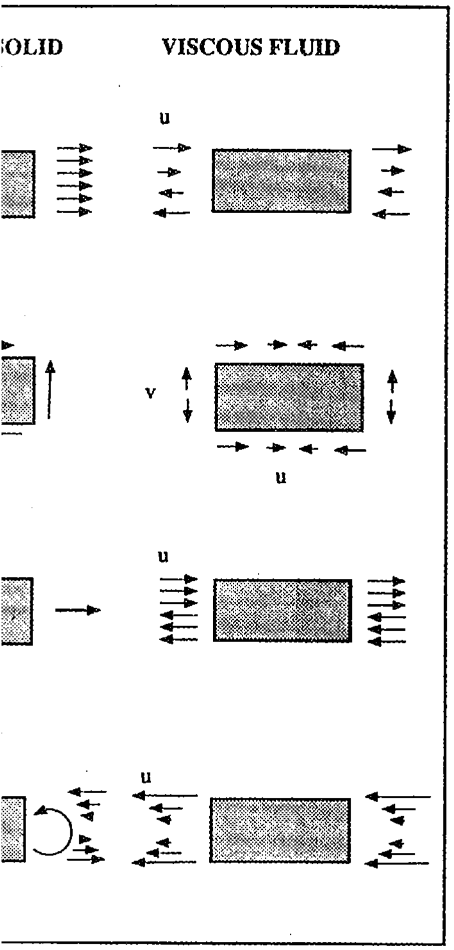

conditions.

3. 0 PHOENICS Settings

3.1 SATELLITE

The Q1 file for the sample problem is included in Appendix 1. The coding is straightforward. A uniform Cartesian grid was employed in all cases. The field variables which are solved for, are pressure, P1, and velocity components, U1 and V1. Storage is also allocated for the velocity gradients (DUX, DUY, DVX, DVY), and the von Mises equivalent stress, VONM, defined below. The U1 and V1 convection terms are deactivated in Group 8. The kinematic viscosity, ENUL, and density, RHO1, are set to unity in Group 9.

Boundary conditions are set, as follows, in Group 13: Mass flux boundary conditions are prescribed on the East and West faces, so that the flow is in through the upper half of the plate, and out of the lower half [see Figure 2(c)]. Since convection is not present, axial diffusion cannot be neglected, and therefore diffusion (ie. wall-type) boundary conditions are prescribed for both U1, and V1. Note that, due to the staggered grid, the axial coefficients are set to two (2), rather than unity, for the cross-wise components. Pressure is fixed at the centre of the domain to zero.

3.2 GROUND

The GROUND module for this project is attached to Appendix 1. Very few modifications are required to this program. At the start of the time step (Group 19. Section 1) a file is opened to allow for monitoring of stress data. At the finish of each sweep (Group 19. Section 7, stresses are calculated provided ISWEEP is a multiple of TSTSWP, in subroutine CALCSTRESS. The normal and shear stresses are calculated using; the GROUND functions DUDX, DUDY, DVDX, DVDY as,

$$\left(\sigma_{xx}\right)_P = \frac{u_e - u_{eS}}{|\overrightarrow{P-S}|} \tag{15}$$

$$\left(\sigma_{yy}\right)_P = \frac{v_n - v_{nE}}{|\overrightarrow{P-E}|} \tag{16}$$

$$\left(\sigma_{xy}\right)_P = \frac{1}{2}\left(\frac{u_e - u_w}{|\vec{e-w}|} + \frac{v_n - v_s}{|\vec{n-s}|}\right) \tag{17}$$

These stresses were then used to calculate the von Mises equivalent stress, σ', which is a commonly-used scalar representation of the stress at a point. It is defined as,

$$\sigma' = \sqrt{\frac{1}{2}\left[\left(\sigma_{xx} - \sigma_{yy}\right)^2 + \sigma_{xx}^2 + \sigma_{yy}^2\right] + 3\sigma_{xy}^2} \tag{18}$$

The von Mises stress was stored as a field variable. Values of σ' at the monitor point were output to the computer screen, and to the file CONVERG.DAT, to provide information on the progress of the simulation

$$\left(\sigma_{xy}\right)_P = \frac{1}{2}\left(\frac{u_e-u_w}{|\overrightarrow{e-w}|} + \frac{v_n-v_s}{|\overrightarrow{n-s}|}\right) \qquad (17)$$

ed to calculate the von Mises equivalent stress, σ', which is a esentation of the stress at a point. It is defined as,

$$\sqrt{\frac{1}{2}\left[\left(\sigma_{xx}-\sigma_{yy}\right)^2+\sigma_{xx}^2+\sigma_{yy}^2\right]+3\sigma_{xy}^2} \qquad (18)$$

stored as a field variable. Values of σ' at the monitor point :r screen, and to the file CONVERG.DAT, to provide infor- ie simulation

4. 0 RESULTS

The problem was simulated using six grids varying in mesh density from 20 x 10 to 140 x 70. Identical grids were utilized when solving the problem by means of the NISA2 FEA package. The results of this study are summarized in Figures 3 to 8 inclusive.

4.1 Typical results

Figures 3 - 5 show typical result obtained using the PHOENICS computer code. Figure 3 shows the velocity distribution for the results obtained using PHOENICS with a 20 x 10 grid over the whole domain.

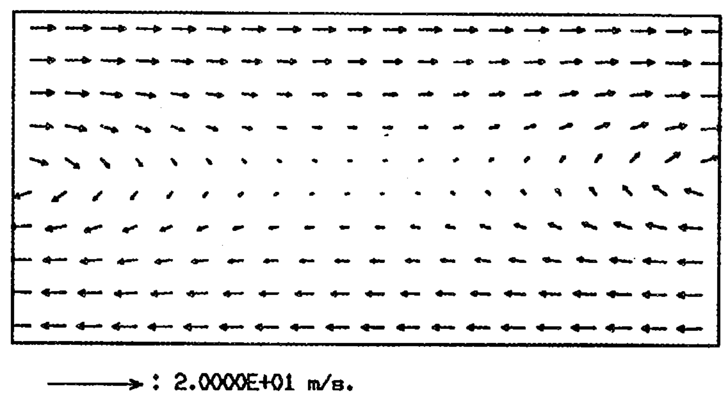

Figure 3. Velocity vectors, PHOENICS.

Figure 4 is a contour plot of the pressure distribution for one half of the plate using a 140 x 70 grid.

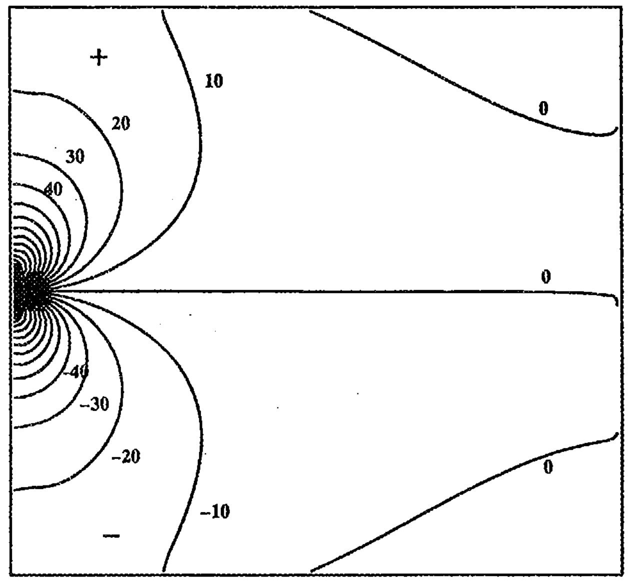

Figure 4. Pressure contours, PHOENICS.

Figure 5 shows contours of von Mises equivalent stress results for one half of the plate, as obtained using PHOENICS (140 x 70 grid). Note the characteristic "birds-eye" pattern with a single pole at the location corresponding to the point-of-application of the force. Almost identical plots were obtained from the results of the NISA2 simulation (see Beale and Elias, 1990).

ıressure distribution for one half of the plate using a

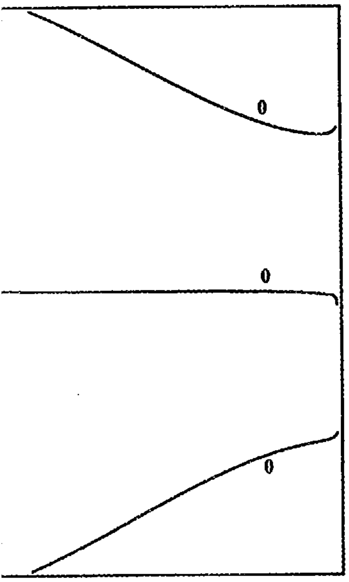

HOENICS.

Mises equivalent stress results for one half of the plate, 40 x 70 grid). Note the characteristic "birds-eye" pattern ation corresponding to the point-of-application of the e obtained from the results of the NISA2 simulation

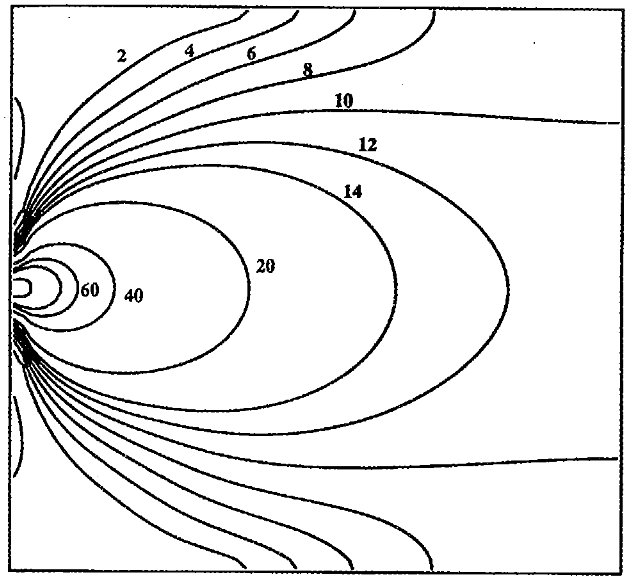

Figure 5. **Von Mises stress contours, PHOENICS.**

4.2 Convergence

Figure 6 shows the value of the von Mises stress at the monitor location corresponding to x* = 0.15, along the plate centreline. The distance, x*, has been normalized with respect to the plate width, L. It can be seen that in all cases, convergence was achieved. With the 20 x 10 grid, full convergence was achieved within 100 - 200 sweeps, while 1000 - 2000 sweeps were required to obtain a fully-converged solution for the finest grid used in this study (140 x 70). It should be noticed that, in all cases, convergence is asymptotic, so that fairly good (within 10%) results were obtained in a fraction of the time required for complete convergence.

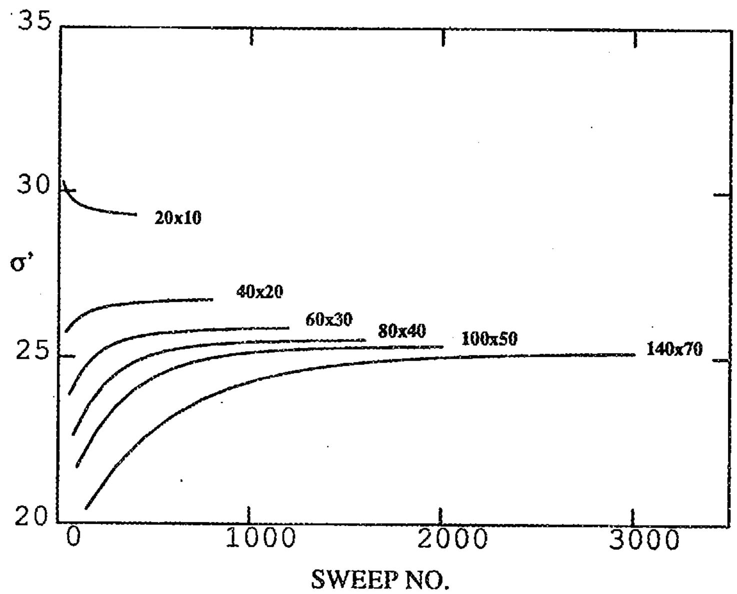

Figure 6. Von Mises stress vs. sweep number at the monitor location, PHOENICS

Grid independence tests were conducted as a part of this programme of research. Figure 7 is a comparison of the von Mises stress vs. non-dimensional distance, x^*, along the plate centreline, for the coarsest (20 x 10) and finest (140 x 70) of the grids employed using PHOENICS, compared to the fine-grid results obtained with the NISA2 program. It can be seen that the results of the PHOENICS simulations are in excellent agreement with those obtained using NISA2, except for values of x^* less than 0.05 - 0.1, where only the fine-grid PHOENICS results shows good agreement with those obtained by means of the FEA code. Values of σ' obtained using grids of intermediate density were located between the values shown in Fig. 7. (the two limiting cases), and have therefore been excluded in this interests of clarity.

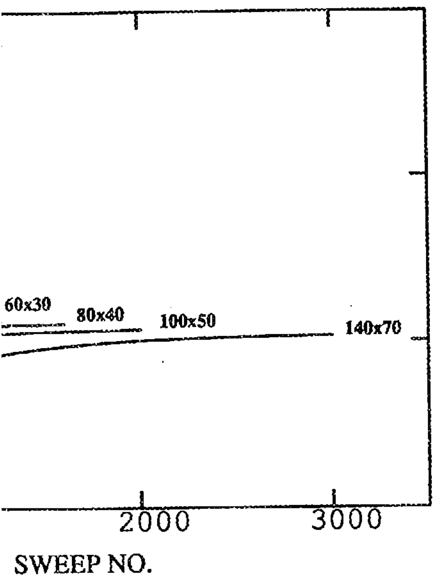

weep number at the monitor location,

ucted as a part of this programme of research. Figure
:s stress vs. non-dimensional distance, x*, along the
20 x 10) and finest (140 x 70) of the grids employed
ıe fine-grid results obtained with the NISA2 program.
e PHOENICS simulations are in excellent agreement
, except for values of x* less than 0.05 - 0.1, where
:sults shows good agreement with those obtained by
σ' obtained using grids of intermediate density were
in Fig. 7. (the two limiting cases), and have therefore
larity.

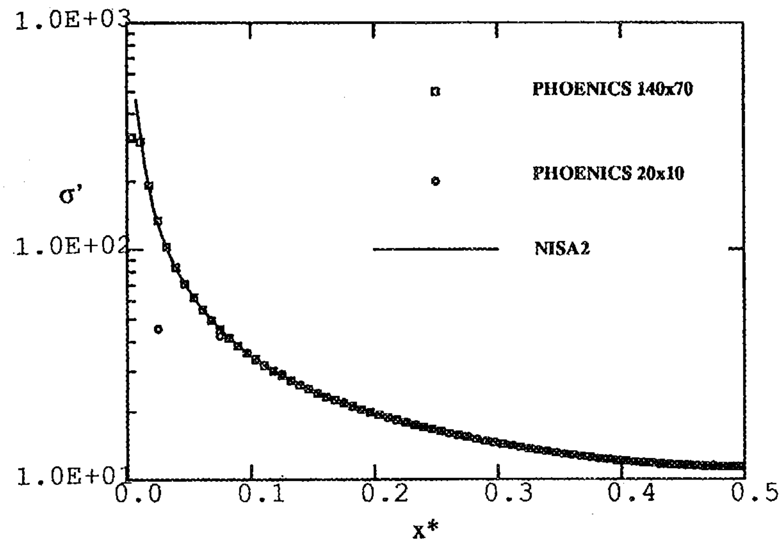

Figure 7. Von Mises stress vs. non-dimensional distance along the plate centreline, PHOENICS and NISA2.

Figure 8 shows values of von Mises stress at the monitor location, $x^* = 0.15$, for both the PHOENICS and NISA2 results, for all of the grids used in this study. It can be seen that both codes converge. At first sight, values of σ' obtained using PHOENICS appear to be substantially more affected by grid size than those obtained using NISA2. However, in the case of PHOENICS, the true location of the monitor point corresponds to the location of the cell corner, as opposed to the cell centre (it being impossible to have the monitor point located at the cell node for both PHOENICS and NISA2).

When corrected (by interpolation) values are plotted [Fig. 8], the PHOENICS results exhibit much less grid dependence. Corrected values obtained with a 20x10 grid are within 4.1% of the results obtained with the finest grids, while those obtained with a 40x20 grid are within 1.2 % of the value of σ' obtained with the 140x70 grid. In the case of NISA2, all the results are within 0.7% of the final converged solution. Agreement between values of σ' at the monitor location obtained with the two codes is 0.2%, for the finest grid used in the study.

The reader will note that although identical grids were used in this study, NISA2 allowed for zero displacement boundary conditions to be prescribed. Since the stress distribution is symmetric in the x direction, only one-half of the domain needed to be simulated, thereby allowing for a reduction by a factor of two, in the size of the NISA2 grids.

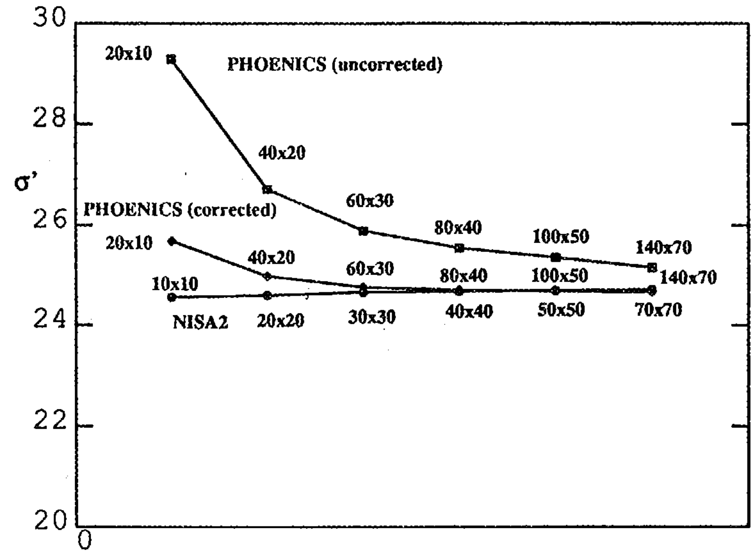

Figure 8. Von Mises stress vs. grid size at the monitor location, PHOENICS and NISA2

location obtained with the two codes is 0.2%, for the

;h identical grids were used in this study, NISA2 al-
dary conditions to be prescribed. Since the stress dis-
:ction, only one-half of the domain needed to be simu-
:tion by a factor of two, in the size of the NISA2 grids.

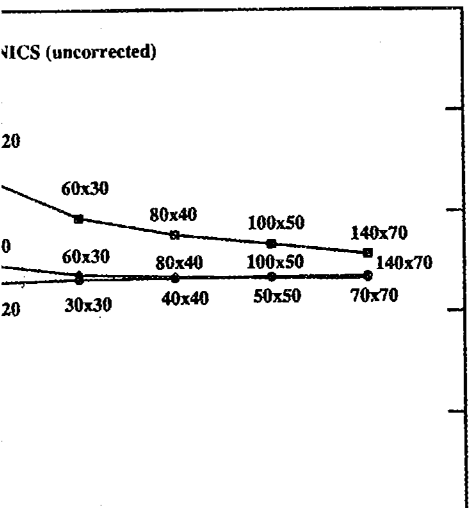

. grid size at the monitor location, PHOENICS and

5. 0 DISCUSSION

Examination of the flow-field shows that the point-of-application of the force may be considered to represent a "pivot-point" around which the fluid is constrained to flow. The symmetry exhibited in both the velocity distribution [Fig. 3] and the pressure field [Fig. 4] is characteristic of creeping flows, which are reversible. The reader will note that there is an element of arbitrariness involved in the magnitude of the reference boundary velocities; it is the velocity gradient rather than the speed which prescribe the state of stress in the plate. In this context, both velocity and pressure are relative quantities.

Inspection of Figure 4 shows the pressure distribution to be in the form of a dipole near to the point-of-application of the force: From complex variable theory, it is known that the application of a force at a point in an elastic solid corresponds, mathematically, to a doublet in the complex potential, W [Eq. 5]. Since the magnitude of the pressure is proportional to the imaginary part of this quantity, it can be seen that this pressure distribution is in fact entirely to be expected. The polarity of the doublet in the right-half of the plate (not shown in Fig. 4) is reversed, as might be anticipated from the inversion of the direction of flow [Fig. 3] in this half of the plate.

Figure 5 shows the distribution of von Mises stress in one-half of the plate as obtained using PHOENICS (the FEA results were essentially the same) It can be seen that von Mises stress approaches infinity at the point-of-application of the force. The von Mises stress is not zero at the plate edge, since even though the stress components corresponding to the normal and shear components of the surface traction must be zero, the component acting on a plane perpendicular to the boundary plane need not be so. The numerically-generated von Mises stress distributions are also in agreement with the results of experimental work, such as the photo-elastic studies of Durelli et. al. (1958).

The centerline stress distribution, as illustrated in Figure 7, suggests that the finite-domain solution behaves well over the majority of the plate even for the coarsest grid used in this study. When, however, x^* is small, the use of finer grids is required in order to prevent stress values being too low. This is not surprising, in view of the highly non-linear nature of the stress distribution, resulting from the presence of a "jump" in the velocity, and the double pole in the pressure field. The prescription of a singular force is of course a theoretical limit which could not be attained in practice, and it would be reasonable to assume that stress boundary conditions would not require the same local concentration of grid cells.

In examining the numerical behaviour of the solution, the von Mises stress in one cell was monitored, the location of this cell corresponding to a distance, x*, of 0.15 from the plate edge, along the centreline. This location was considered appropriate owing to the proximity to a high stress area, being surrounded by a zone where the stress-gradient varies significantly. It is evident from Figure 8 that grid independence has been reached for all but the coarsest grids used in this project. It can also be seen from Figure 8, that the finite-domain-based PHOENICS solutions appear to be only slightly more dependent on grid size than those based on the FEA code NISA2. The choice of monitor location is clearly of some importance.

No difficulty was experienced in obtaining convergent solutions using the finite-domain method, however, the grid dependence tests did show that grid size has an appreciable effect on the number of sweeps required to obtain a fully-converged solution (and therefore computer costs). One hundred sweeps on a 20 x 10 grid required 40 (DEC VAXstation 3200) CPU seconds, while a similar number of sweeps on a 200 x 100 grid required 1.4 CPU hour. These numbers both represent approximately 0.2 CPU seconds per cell for 100 sweeps. In view of the marginal improvements in terms of results, the extra cost associated with finer grids does not appear to be justified.

Although the FEA-based NISA2 code was run using a different computer (IBM VM 3090) rather than the SIMPLE-based PHOENICS (VAX 3100 and 3200), existing benchmarks allow rudimentary comparison of the computing costs required for the two cases to be made. It is estimated that[1] NISA2 required an equivalent of 0.1 VAX CPU seconds per cell to reach a final solution. This value was found to be relatively independent of grid size. Since the finite-domain solutions required between 100 and 200 sweeps for full solution, it may be concluded that the two methods are very roughly comparable in speed, when applied to coarse grids of the same size. It is however apparent that, for the problem under consideration, if very precise results are required near to the location of the force, then there is a performance penalty associated with the PHOENICS, due to the relatively large number of sweeps required to obtain a solution using a fine grid. Under these circumstances, the use of power-law type grids is recommended.

In this study, values of the boundary velocities were prescribed as if they acted at the faces of the appropriate cells, the momentum equation source-term coefficients being set according to the diffusion formula. For problems involving more complex geometrical boundaries, a general integration procedure to calculate the values of the boundary velocities from the prescribed surface tractions is cumbersome. Consider, for example, a cylindrical element subject to a radial stress, σ_r. As was pointed by Goodier (1934), the

[1] Based on the RETEST benchmark test, showing an IBM 3090 to have an estimated speed of 15.3 times that of a VAXstation 3200.

viour of the solution, the von Mises stress in one cell is cell corresponding to a distance, x*, of 0.15 from the This location was considered appropriate owing to the being surrounded by a zone where the stress-gradient dent from Figure 8 that grid independence has been ids used in this project. It can also be seen from Figure IOENICS solutions appear to be only slightly more de- based on the FEA code NISA2. The choice of monitor tance.

obtaining convergent solutions using the finite-domain idence tests did show that grid size has an appreciable equired to obtain a fully-converged solution (and there- d sweeps on a 20 x 10 grid required 40 (DEC VAXsta- a similar number of sweeps on a 200 x 100 grid re- bers both represent approximately 0.2 CPU seconds per he marginal improvements in terms of results, the extra oes not appear to be justified.

2 code was run using a different computer (IBM VM -based PHOENICS (VAX 3100 and 3200), existing comparison of the computing costs required for the two that[1] NISA2 required an equivalent of 0.1 VAX CPU solution. This value was found to be relatively inde- finite-domain solutions required between 100 and 200 be concluded that the two methods are very roughly ed to coarse grids of the same size. It is however appar- onsideration, if very precise results are required near to there is a performance penalty associated with the y large number of sweeps required to obtain a solution rcumstances, the use of power-law type grids is recom-

ndary velocities were prescribed as if they acted at the momentum equation source-term coefficients being set ila. For problems involving more complex geometrical n procedure to calculate the values of the boundary ve- face tractions is cumbersome. Consider, for example, a radial stress, σ_r. As was pointed by Goodier (1934), the

it, showing an IBM 3090 to have an estimated speed of 15.3 times

fluid analogue is a constant angular velocity v_t (not constant $\partial v_r/\partial t$ as might be expected). This does not imply that it is not possible to write boundary conditions in general curvilinear coordinates, but further research is needed.

An alternative method of prescribing momentum boundary conditions is to specify fixed sources of velocity fluxes (ie. gradients). From Table 1, it is seen that prescription of a shear stress, σ_t, on say the east face, is equivalent to a flux of normal velocity in the normal direction, $\partial u/\partial x$ Although the prescription of a normal stress σ_n corresponds to a velocity gradient in the tangential direction, $\partial u/\partial y$, this can easily be converted to a flux of the form, $\partial v/\partial x$, using the fact that the sum of the convection terms is zero. Time constraints prevented any investigation into this possibility from be included in this paper.

Up to this point, no mention has been made of strains and displacements. These were not calculated as a part of this study, however, guidelines for the computation of these quantities are discussed below: Normal and shear strains, ε_{xx}, ε_{yy}, ε_{xy}, may be calculated directly from the stress components, σ_{xx}, σ_{yy}, σ_{xy}, using the well-known constitutive equations for a linear elastic solid (generalized Hookes' Law). The constitutive assumption made (ie. plane stress or plane strain) will affect only the strain distribution and not the stress field. Displacements may then be obtained using a simple difference procedure. Consider, for example, the x-direction displacement, U_x, which may be written in terms of its east and north neighbours as,

$$\frac{(U_x)_E - (U_x)_P}{|\vec{PE}|} = (\epsilon_{xx})_P \tag{19}$$

$$\frac{(U_x)_N - (U_x)_P}{|\vec{PN}|} = (\epsilon_{xy})_P \tag{20}$$

Similar relations may be written for U_x in terms of the south and east neighbours. The displacement field, U_x, may then be obtained either; (a) at the end of the simulation by "integrating" from a reference point located e.g. in the south-west corner of the domain using Equations (19) and (20), or (b) by constructing a finite-difference equation in terms of all four neighbours of U_x, and solving iteratively throughout the simulation. The former approach would be suitable for simple geometries with prescribed stress or force boundary conditions, while the latter may be required for complex multiply-connected regions, or for problems where there are displacement boundary conditions.

Although (a) above is simpler, there are a number of reasons why it may be useful to calculate displacements throughout the simulation using (b). For example, lines of stress symmetry do not correspond to velocity symmetry conditions. It was not, therefore, possible to take advantage of geometric symmetry in PHOENICS, and it was for this reason that the grids constructed for use in PHOENICS were twice as large as those used in the NISA2 simulations. In order to take advantage of symmetry, a method of prescribing zero displacement boundary conditions is needed. In this regard, some sort of iterative procedure, whereby, the velocity gradients could be corrected, until they effect zero-displacements along the appropriate boundary is probably required. Since, in general, both displacement and force boundary conditions are to be anticipated, this procedure, while obviously necessitating an increase in computation time and storage, may ultimately prove necessary.

The methodology described here may be readily extended to problems involving the use of a body-fitted coordinate (BFC) grid. For cases involving orthogonal grids, the stress components (in the local coordinate directions) may be calculated using the simplified relations of Equations (15) - (17). The reader will note the fluid vorticity, ζ, corresponds to the sum of the normal elastic stresses. Since it is well known that the sum of the normal stresses is independent of the coordinate system (e.g. by constructing Mohr's circle), the vorticity and hence the pressure distribution are coordinate independent. Since von Mises stress is based on an invariant of the stress tensor (Hunter, 1983), this derived quantity may also be calculated using Equation (18), from the in-cell stress components in the local curvilinear coordinate directions [Eqs. (15) -(17)], provided the grid is orthogonal. In cases where there is significant non-orthogonality, however, it is evident that Equations (15) - (17) may not be used to calculate the stress components, as the covariant derivatives of the velocity vector can no longer be computed using a simple difference scheme. A discussion of non-orthogonal effects is beyond the scope of this report.

It must be stated that the authors did consider an example involving a square plate with a circular hole, involving the use of an O-type BFC grid. Good result were obtained near the hole, however towards the outer corners unrealistic pressure (and hence stress) distributions were obtained. This was probably due to the simplified formulation of the diffusion-flux terms in PHOENICS version 1.4 (time prevented an investigation of the improved formulation inherent in version 1.5, in time for inclusion in this paper). The authors also simulated all of the examples given in Figure 2 for a square plate (constant normal and shear stress, and bending moment boundary conditions) in Cartesian coordinates. For these cases, the resulting stress distributions are constant or one-dimensional, (ie. rather uninteresting), and were therefore excluded from this text of this report. It should, however be noted that results obtained for these cases were excellent.

there are a number of reasons why it may be useful to
ɔut the simulation using (b). For example, lines of stress
ı velocity symmetry conditions. It was not, therefore,
eometric symmetry in PHOENICS, and it was for this
d for use in PHOENICS were twice as large as those
In order to take advantage of symmetry, a method of
ɔundary conditions is needed. In this regard, some sort
the velocity gradients could be corrected, until they ef-
ıe appropriate boundary is probably required. Since, in
'orce boundary conditions are to be anticipated, this pro-
:ating an increase in computation time and storage, may

: may be readily extended to problems involving the use
Ͻ) grid. For cases involving orthogonal grids, the stress
nate directions) may be calculated using the simplified
17). The reader will note the fluid vorticity, ζ, corre-
l elastic stresses. Since it is well known that the sum of
nt of the coordinate system (e.g. by constructing Mohr's
the pressure distribution are coordinate independent.
on an invariant of the stress tensor (Hunter, 1983), this
culated using Equation (18), from the in-cell stress com-
:oordinate directions [Eqs. (15) -(17)], provided the grid
ıere is significant non-orthogonality, however, it is evi-
may not be used to calculate the stress components, as
velocity vector can no longer be computed using a sim-
ssion of non-orthogonal effects is beyond the scope of

; did consider an example involving a square plate with
se of an O-type BFC grid. Good result were obtained
the outer corners unrealistic pressure (and hence stress)
s was probably due to the simplified formulation of the
ICS version 1.4 (time prevented an investigation of the
in version 1.5, in time for inclusion in this paper). The
examples given in Figure 2 for a square plate (constant
ıding moment boundary conditions) in Cartesian coordi-
ting stress distributions are constant or one-dimensional,
vere therefore excluded from this text of this report. It
esults obtained for these cases were excellent.

The rationale used in this project involved the transformation of the equations of compatibility and equilibrium for a linear elastic solid [Eqs. (1) - (3)] to the pressure- linked Stokes' equations, [Eqs. (7) - (9)]. These were then discretized and solved by means of the PHOENICS code which is based on a variant of the SIMPLE algorithm (Patankar and Spalding, 1972). Other CFD algorithms could also be employed to the same end: For instance, the stream function-vorticity method (Runchal et. al., 1969) would allow for the direct solution of the stress function ϕ and the harmonic function η, without the need to iterate on the coupled pressure and velocity fields. (The main difficulty associated with this approach is the prescription of boundary conditions)

It is, of course, true that FEA and other methods are already capable of solving complex structural analysis problems, efficiently. It would be wrong, however, to conclude that there is little point to attempting to achieve the same end by means of CFD algorithms. The scope of this project was confined to demonstrating how a CFD code could be used to solve elementary stress analysis problems. Having shown that this is the case, there still remains the more important (and more complex) problem of "conjugate" structural/fluid-flow analysis, ie. the solution of problems involving both fluid flow and stress analysis simultaneously, e.g. the stress distribution in an object mounted in a wind-tunnel. Applications requiring analyses of this type are numerous and can be found in several diverse industries; pressure vessel design, analysis of ship's hulls, problems in aero-elasticity, metal casting, and nuclear reactor safety, to name but a few. At present, engineers seeking to analyze both fluid-flow and structural details of a design are forced to use different codes to achieve this end. This often requires complicated manipulations of grids and field data. From a purely pragmatic point-of-view, the use of a single code to conduct both analyses is highly desirable.

It is believed that the methodology described in this report could, with some effort, be extended to solve problems in this class: Solid and fluid regions could be isolated by removing appropriate linkages in the finite domain equations in Group 8. Conventional 'wall-type' boundary conditions would be applied to the flow on the fluid side of the solid-fluid interface; the resulting fluid pressure and velocity fields could then be used to compute the normal and shear stresses acting on the solid object, on a per sweep basis. The stress distribution in the solid would then be computed using the method described in this paper, with convection being cut out by way of GROUND. The reader will note that, since linear elasticity theory is based on the premise of small deformation, the solid-fluid interface is fixed so that even though the flow-field affects the stress distribution in the solid, the converse is not true.

The methods described in this paper can be used to solve problems involving biaxial stress distributions. Unfortunately, it is not possible to mathematically extend the solid-fluid analogy to problems involving triaxial stress distributions. This does not necessarily preclude the solution of 3-D problems. One possible line-of-attack might be to consider the stress distribution in each cell as if it were made up of three locally-plane-stress (or alternatively locally-plane-strain) distributions corresponding to planes perpendicular to the three coordinate directions. This type of assumption is in many ways similar to the conventional CFD assumption, namely that the total (convective plus diffusive) flux is made up of three locally independent one-dimensional fluxes; the latter giving rise to the well-known phenomenon of false diffusion. At this stage, however, it must be admitted that the use of SIMPLE-type algorithms to solve problems involving triaxial stresses is the subject of speculation.

There are, of course, a number of engineering problems where the assumptions of (generalized) plane stress or plane strain are entirely reasonable, so that the rationale presented in this report can be directly applied. Examples include, the flow around high aspect-ratio airfoils, flow inside thin-walled pressure vessels, or around immersed objects where the flow is oriented in a particular direction. Problems involving axisymmetric stress distributions create no significant difficulties, while the presence of body forces and/or thermo-elastic stresses can be dealt with by introducing appropriate volumetric source terms, and in the latter case solving by solving for enthalpy in addition to momentum. While it has ostensively been shown that the methods of CFD may be directly applied to certain classes of problem in linear elasticity, there is clearly much scope for further research in this area.

:h cell as if it were made up of three locally-plane-stress rain) distributions corresponding to planes perpendicu- ons. This type of assumption is in many ways similar to ɔn, namely that the total (convective plus diffusive) flux ɔendent one-dimensional fluxes; the latter giving rise to false diffusion. At this stage, however, it must be admit- ype algorithms to solve problems involving triaxial tion.

ɪf engineering problems where the assumptions of (gen- train are entirely reasonable, so that the rationale pre- ectly applied. Examples include, the flow around high thin-walled pressure vessels, or around immersed ob- n a particular direction. Problems involving axisymmet- o significant difficulties, while the presence of body sses can be dealt with by introducing appropriate volu- latter case solving by solving for enthalpy in addition to ively been shown that the methods of CFD may be di- s of problem in linear elasticity, there is clearly much area.

6. 0 CONCLUSIONS AND RECOMMENDATIONS

The analogy between plane creeping fluid-flow and two-dimensional linear elasticity was discussed. In the analogue, fluid velocity gradients correspond to solid stresses, so that fluid vorticity is associated with (the negative of) the sum of the normal stresses. Typical solid mechanics loading conditions were considered, as if they were fluid boundary conditions: It was shown that normal and shear stresses, forces, and bending moments could all be written in terms of fluid boundary conditions.

The case of a rectangular plate subject to uniaxial force loading was considered in detail, and the results obtained using the PHOENICS program were compared to those obtained with the FEA code NISA2, with excellent results. Grid dependence studies showed the CFD solution to be only slightly more dependent on grid size than the FEA solutions.

Further extensions to this CFD-based methodology are possible, and should be considered: These include the use of CFD techniques to solve problems involving triaxial stress distributions, the influence of body forces, and problems in linear thermoelasticity. In this program of research, only stress-related boundary conditions were considered. A technique whereby the stress distribution resulting from zero displacement boundary conditions could be ascertained, would result in economy when solving problems exhibiting stress symmetry, and is prerequisite to the solution of problems involving displacement or mixed boundary conditions.

Probably the area of greatest promise for the techniques described in this report, lies in the solution of problems requiring conjugate structural/fluid-flow analysis. The development of a single computer code to simultaneously analyze both the fluid-flow, and stress distribution in complex components would represent a significant advance in the science of computational fluid dynamics. Uses for such code are manifold.

7. 0 NOMENCLATURE

Symbol		Units
F	Body force	(N)
I	Moment of inertia	(m^4)
L	Plate width	(m)
M	Bending moment	(N.m)
p	Fluid pressure	(N/m^2)
U	Displacement	(m/m)
u	Velocity component	(m/s)
v	Velocity component	(m/s)
W	Complex harmonic function	
x	Coordinate distance, distance from neutral axis	(m)
x*	Non-dimensional distance	(-)
y	Coordinate distance, distance from neutral axis	(m)
ε	Strain	(m/m)
ξ	Harmonic function	(kg/ms^2)
η	Harmonic function	(kg/ms^2)
μ	Coefficient of viscosity	($N.s/m^2$)
ζ	Vorticity	(s^{-1})
ρ	Density	(kg/m^3)
σ	Stress	(N/m^2)
σ'	Von Mises equivalent stress	(N/m^2)
ϕ	Airy's stress function	($kg.m^2/s^2$)
ψ	Stream function	(m^3/s)

Subscripts

e	East cell interface
E	East cell centre
n	North cell interface, normal
N	North cell centre
P	Cell centre
p	Pressure, mass
r	Radial
s	South cell interface
S	South cell centre
t	Tangential

	Units
	(N)
	(m^4)
	(m)
	(N.m)
	(N/m^2)
	(m/m)
	(m/s)
	(m/s)
unction	
, distance from neutral axis	(m)
stance	(-)
, distance from neutral axis	(m)
	(m/m)
	(kg/ms^2)
	(kg/ms^2)
sity	($N.s/m^2$)
	(s^{-1})
	(kg/m^3)
	(N/m^2)
nt stress	(N/m^2)
n	($kg.m^2/s^2$)
	(m^3/s)

, normal

w	West cell interface
W	West cell centre
u	u velocity
v	v velocity
x	x direction
y	y direction

Superscripts

b	Bending

8. 0 REFERENCES

1. Beale, S.B, and Elias, S.J. Numerical Solution of Two-dimensional Elasticity Problems by Means of a "SIMPLE"-based Finite-difference Scheme. Institute for Mechanical Engineering. National Research Council, Ottawa, Ont. TR-LT-020 (NRC No. 32090), 1990.
2. Chou, P.C. and Pagano, N.J. Elasticity. D. Van Nostrand Co. Princeton, 1967.
3. Dean, W.R.. An Application in Hydrodynamics of the Green's Function of an Elastic Plate. Mathematika, Vol 5., pp. 85-92, December 1958.
4. Durelli, A.J., Phillips, E.A. and Tsao, C.H. Introduction to the Theoretical and Experimental Analysis of Stress and Strain. McGraw-Hill Book Company, New York, 1958.
5. Goodier, J.N. An Analogy Between the Slow Motions of a Viscous Fluid in Two Dimensions, and Systems of Plane Stress. Phil. Mag., Vol. 17, pp. 554-576, March 1934.
6. Hunter, S.C., Mechanics of Continuous Media. Ellis Horwood Ltd., Chichester, 1983.
7. Johnston, J.Z. and Tabarrok, B. Stream Function - Stress Function Approach to Incompressible Flows. Proc. of the First International Conference of Numerical Methods in Laminar and Turbulent Flow. pp. 81-88, Pentech Press, London, July 1978.
8. Langlois, W.E. Slow Viscous Flow. The MacMillan Company, New York, 1964.
9. Little, R.W. Elasticity. Prentice-Hall, Inc., Englewood Cliffs, New Jersey, 1973.
10. Mathers, M.D. (ed.). NISA User's Manual, Release 83.1. Engineering Mechanics Research Corporation, Troy, Michigan, 1983.
11. Muskhelishivili, N.I.. Some Basic Problems of the Mathematical Theory of Elasticity. P. Noordhoff Ltd., Groningen, Holland, 1953.
12. Patankar, S.V. and Spalding, D.B. A Calculation Procedure for Heat, Mass and Momentum Transfer in Three-Dimensional Parabolic Flows. Int. J. of Heat and Mass Transfer, Vol. 15, pp. 1787-1806, 1972.
13. Runchal, A.K., Spalding, D.B. and Wolfshtein, M. Numerical Solution of the Elliptic Equations for Transport of Vorticity, Heat, and Matter in Two-Dimensional Flow. High Speed Computing in Fluid Dynamics, The Physics of Fluids Supplement II, pp. 21-28, 1969.
14. Timoshenko, S. Theory of Elasticity. McGraw-Hill Book Company, New York, 1934.

ərical Solution of Two-dimensional Elasticity Prob-
'-based Finite-difference Scheme. Institute for Me-
Research Council, Ottawa, Ont. TR-LT-020 (NRC

sticity. D. Van Nostrand Co. Princeton, 1967.

Iydrodynamics of the Green's Function of an Elas-
p. 85-92, December 1958.

Tsao, C.H. Introduction to the Theoretical and Ex-
d Strain. McGraw-Hill Book Company, New York,

ɾeen the Slow Motions of a Viscous Fluid in Two
ne Stress. Phil. Mag., Vol. 17, pp. 554-576, March

ntinuous Media. Ellis Horwood Ltd., Chichester,

Stream Function - Stress Function Approach to In-
; First International Conference of Numerical Meth-
low. pp. 81-88, Pentech Press, London, July 1978.

ow. The MacMillan Company, New York, 1964.

Hall, Inc., Englewood Cliffs, New Jersey, 1973.

ɾ's Manual, Release 83.1. Engineering Mechanics
chigan, 1983.

ic Problems of the Mathematical Theory of Elastic-
n, Holland, 1953.

B. A Calculation Procedure for Heat, Mass and Mo-
ensional Parabolic Flows. Int. J. of Heat and Mass
'6, 1972.

ınd Wolfshtein, M. Numerical Solution of the Ellip-
Vorticity, Heat, and Matter in Two-Dimensional
in Fluid Dynamics, The Physics of Fluids Supple-

sticity. McGraw-Hill Book Company, New York,

APPENDIX 1.

Q1 Listing

```
TALK=F;RUN( 1, 1);VDU=DEC GKS
  GROUP 1. Run title and other preliminaries
TEXT(Stress on a plate)
REAL(RXMON)
  GROUP 2. Transience; time-step specification
STEADY=T
  GROUP 3. X-direction grid specification
GRDPWR(X,140,2.,1.)
  GROUP 4. Y-direction grid specification
GRDPWR(Y,70,1.,1.)
  GROUP 5. Z-direction grid specification
  GROUP 6. Body-fitted coordinates or grid distortion
  GROUP 7. Variables stored, solved & named
SOLVE(U1,V1,P1)
SOLUTN(P1,Y,Y,Y,N,N,N)
STORE(DUX,DUY,DVX,DVY,VONM)
  GROUP 8. Terms (in differential equations) & devices
TERMS(U1,Y,N,Y,N,P,P)
TERMS(V1,Y,N,Y,N,P,P)
  GROUP 9. Properties of the medium (or media)
ENUL=1;RHO1=1
  GROUP 10. Inter-phase-transfer processes and properties
  GROUP 11. Initialization of variable or porosity fields
FIINIT(P1)=0;FIINIT(U1)=0;FIINIT(V1)=0
  RESTRT(ALL)
  GROUP 12. Convection and diffusion adjustments
  GROUP 13. Boundary conditions and special sources
PATCH(W1A,WWALL,1,1,1,NY/2,1,NZ,1,LSTEP)
PATCH(W1B,WWALL,1,1,1,NY/2,1,NZ,1,LSTEP)
PATCH(W1C,WEST,1,1,1,NY/2,1,NZ,1,LSTEP)
COVAL(W1A,V1,1,0.)
COVAL(W1B,U1,2.,-5.)
COVAL(W1C,P1,FIXFLU,-5.)

PATCH(W2A,WWALL,1,1,NY/2+1,NY,1,NZ,1,LSTEP)
PATCH(W2B,WWALL,1,1,NY/2+1,NY,1,NZ,1,LSTEP)
PATCH(W2C,WEST,1,1,NY/2+1,NY,1,NZ,1,LSTEP)
COVAL(W2A,V1,1,0.)
COVAL(W2B,U1,2.,5.)
```

```
COVAL(W2C,P1,FIXFLU,5.)

PATCH(N1,NWALL,1,NX,NY,NY,1,NZ,1,LSTEP)
COVAL(N1,U1,1.,5.)

PATCH(S1,SWALL,1,NX,1,1,1,NZ,1,LSTEP)
COVAL(S1,U1,1.,-5.)


PATCH(E1A,EWALL,NX,NX,1,NY/2,1,NZ,1,LSTEP)
PATCH(E1B,EWALL,NX-1,NX-1,1,NY/2,1,NZ,1,LSTEP)
PATCH(E1C,EAST,NX,NX,1,NY/2,1,NZ,1,LSTEP)
COVAL(E1A,V1,1.,0.)
COVAL(E1B,U1,2.,-5.)
COVAL(E1C,P1,FIXFLU,5.)

PATCH(E2A,EWALL,NX,NX,NY/2+1,NY,1,NZ,1,LSTEP)
PATCH(E2B,EWALL,NX-1,NX-1,NY/2+1,NY,1,NZ,1,LSTEP)
PATCH(E2C,EAST,NX,NX,NY/2+1,NY,1,NZ,1,LSTEP)
COVAL(E2A,V1,1.,0.)
COVAL(E2B,U1,2.,5.)
COVAL(E2C,P1,FIXFLU,-5.)

PATCH(FXP,CELL,NX/2,NX/2,NY/2,NY/2,1,NZ,1,LSTEP)
COVAL(FXP,P1,FIXVAL,0.)

  GROUP 14. Downstream pressure for PARAB=.TRUE.
  GROUP 15. Termination of sweeps
LSWEEP = 3000
  GROUP 16. Termination of iterations
  GROUP 17. Under-relaxation devices
RELAX(U1,FALSDT,1.)
RELAX(V1,FALSDT,1.)
VARMAX(P1)=5000
VARMIN(P1)=-5000
VARMAX(U1)=20
VARMIN(U1)=-20
VARMAX(V1)=20
VARMIN(V1)=-20
  GROUP 18. Limits on variables or increments to them
  GROUP 19. Data communicated by satellite to GROUND
USEGRD=T
USEGRX=F
  GROUP 20. Preliminary print-out
```

```
,1,NZ,1,LSTEP)

Z,1,LSTEP)

Y/2,1,NZ,1,LSTEP)
,1,NY/2,1,NZ,1,LSTEP)
2,1,NZ,1,LSTEP)

/2+1,NY,1,NZ,1,LSTEP)
,NY/2+1,NY,1,NZ,1,LSTEP)
+1,NY,1,NZ,1,LSTEP)

Y/2,NY/2,1,NZ,1,LSTEP)

re for PARAB=.TRUE.
eps

itions
vices

or increments to them
d by satellite to GROUND

ut
```



```
  GROUP 21. Print-out of variables
OUTPUT(DUX,N,N,N,N,N,N)
OUTPUT(DUY,N,N,N,N,N,N)
OUTPUT(DVX,N,N,N,N,N,N)
OUTPUT(DVY,N,N,N,N,N,N)
OUTPUT(P1,N,N,Y,N,N,Y)
OUTPUT(U1,N,N,Y,N,N,Y)
OUTPUT(V1,N,N,Y,N,N,Y)
OUTPUT(VONM,Y,N,N,N,Y,N)
  INIFLD = T
  GROUP 22. Spot-value print-out
TSTSWP = LSWEEP/20
RXMON = .15*NX
IXMON = RXMON
IYMON = NY/2
  GROUP 23. Field print-out and plot control
NPLT=TSTSWP;ITABL = 3
  GROUP 24. Dumps for restarts
STOP
```

GROUND Listing

```
C*****************************************************************
C--- GROUP 1. Run title and other preliminaries
C
   1 GO TO (1001,1002),ISC
 1001 CALL MAKE(XU2D)
      CALL MAKE(YV2D)
      CONTINUE
      RETURN
 1002 CONTINUE
      RETURN
C****************************************************************
C--- GROUP 19. Special calls to GROUND from EARTH
C
  19 GO TO (191,192,193,194,195,196,197,198),ISC
  191 CONTINUE
C  * ------------------ SECTION 1 ---- START OF TIME STEP.
      OPEN (UNIT = 71,FILE='CONVERG.DAT',STATUS='NEW')
      WRITE (71,*) ' ISWEEP  VONM '
  192 CONTINUE
C  * ------------------ SECTION 2 ---- START OF SWEEP.
      RETURN
```

```
 193 CONTINUE
C  * ------------------ SECTION 3 ---- START OF IZ SLAB.
   RETURN
 194 CONTINUE
C  * ------------------ SECTION 4 ---- START OF ITERATION.
C
   RETURN
 195 CONTINUE
C  * ------------------ SECTION 5 ---- FINISH OF ITERATION.
   RETURN
 196 CONTINUE
C  * ------------------ SECTION 6 ---- FINISH OF IZ SLAB.
   RETURN
 197 CONTINUE
C  * ------------------ SECTION 7 ---- FINISH OF SWEEP.
c
1971 FORMAT (I4,3X,F7.3)
1972 FORMAT (' ISWEEP ='I4,3X,' VONM =',F11.4)
   IF (MOD(ISWEEP,TSTSWP).EQ.0) THEN
   CALL CALCSTRESS
   IVON = INAME('VONM')
   L0VON=L0F(IVON)
   I = IYMON + (IXMON-1)*NY
   WRITE(71,1971) ISWEEP, F(L0VON+I)
   WRITE(6,1972) ISWEEP, F(L0VON+I)
   END IF
   RETURN
 198 CONTINUE
C  * ------------------ SECTION 8 ---- FINISH OF TIME STEP.
   CLOSE (UNIT = 71)
   RETURN
C*****************************************************************
C SUBROUTINE CALCSTRESS
C
C  Calculates normal, shear and VonMises stress throughout the body
C
   SUBROUTINE CALCSTRESS
   INCLUDE 'GRDLOC'
   COMMON/IDATA/NX,NY
   IDUX = INAME('DUX')
   IDUY = INAME('DUY')
   IDVX = INAME('DVX')
   IDVY = INAME('DVY')
   IVON = INAME('VONM')
```

```
;TART OF IZ SLAB.

START OF ITERATION.

FINISH OF ITERATION.

FINISH OF IZ SLAB.

- FINISH OF SWEEP.

;,' VONM =',F11.4)
Q.0) THEN

,0VON+I)
)VON+I)

---- FINISH OF TIME STEP.

**************************************

VonMises stress throughout the body

SS
```



```
LOVON=L0F(IVON)
LODUX=L0F(IDUX)
LODUY=L0F(IDUY)
LODVX=L0F(IDVX)
LODVY=L0F(IDVY)
CALL FNDUDX(IDUX,U1)
CALL FNDVDX(IDVX,V1)
CALL FNDUDY(IDUY,U1)
CALL FNDVDY(IDVY,V1)
DO IX = 1,NX
DO IY = 1,NY
I = IY + (IX-1)*NY
TAU = (F(LODVY+I) - F(LODUX+I))/2
SX = F(LODUY+I)
SY = -F(LODVX+I)
F(LOVON+I)=SQRT(((SX-SY)**2 + SX**2 + SY**2)/2 + (3*(TAU**2)))
END DO
END DO
RETURN
END
```